

A Genetic Defect in Exportin-5 Traps Precursor MicroRNAs in the Nucleus of Cancer Cells

Sonia A. Melo,^{1,2} Catia Moutinho,¹ Santiago Ropero,³ George A. Calin,⁴ Simona Rossi,⁴ Riccardo Spizzo,⁴ Agustin F. Fernandez,¹ Veronica Davalos,¹ Alberto Villanueva,⁵ Guillermo Montoya,⁶ Hiroyuki Yamamoto,⁷ Simo Schwartz, Jr.,⁸ and Manel Esteller^{1,9,*}

¹Cancer Epigenetics and Biology Program (PEBC), Bellvitge Biomedical Research Institute (IDIBELL), 08907 L'Hospitalet, Barcelona, Catalonia, Spain

²Porto Medical University (FMUP), 4200-319 Porto, Portugal

³Biochemistry Department, Alcala University, 28801 Alcala de Henares, Madrid, Spain

⁴Experimental Therapeutics and The Center for RNA Interference and Non-coding RNAs, MD Anderson Cancer Center, Houston, TX 77030, USA

⁵Translational Research Laboratory, Institut Catala d'Oncologia, 08907 L'Hospitalet, Barcelona, Catalonia, Spain

⁶Macromolecular Crystallography Group, Spanish National Cancer Research Centre (CNIO), 28029 Madrid, Spain

⁷First Department of Internal Medicine, Sapporo Medical University South 1, West 16, Chuo-ku, Sapporo 060-8543, Japan

⁸Molecular Biology and Biochemistry Research Center for Nanomedicine, CIBBIM-Nanomedicine, Vall d'Hebron University Hospital, 08035 Barcelona, Catalonia, Spain

⁹Institucio Catalana de Recerca i Estudis Avançats (ICREA), 08010 Barcelona, Catalonia, Spain

*Correspondence: mesteller@iconcologia.net

DOI 10.1016/j.ccr.2010.09.007

SUMMARY

The global impairment of mature microRNAs (miRNAs) is emerging as a common feature of human tumors. One interesting scenario is that defects in the nuclear export of precursor miRNAs (pre-miRNAs) might occur in transformed cells. Exportin 5 (*XPO5*) mediates pre-miRNA nuclear export and herein we demonstrate the presence of *XPO5*-inactivating mutations in a subset of human tumors with microsatellite instability. The *XPO5* genetic defect traps pre-miRNAs in the nucleus, reduces miRNA processing, and diminishes miRNA-target inhibition. The *XPO5* mutant form lacks a C-terminal region that contributes to the formation of the pre-miRNA/*XPO5*/Ran-GTP ternary complex and pre-miRNAs accumulate in the nucleus. Most importantly, the restoration of *XPO5* functions reverses the impaired export of pre-miRNAs and has tumor-suppressor features.

INTRODUCTION

MicroRNAs (miRNAs) are small noncoding RNAs that regulate gene expression by targeting messenger RNA (mRNA) transcripts. MiRNAs play important roles in several cellular processes by simultaneously controlling the expression levels of hundreds of genes (He and Hannon, 2004; Bartel, 2004; Chang and Mendell, 2007). In human cancer, miRNA expression profiles differ between normal tissues and derived tumors and between tumor types (Lu et al., 2005; Volinia et al., 2006), and it has been shown that miRNAs can act as oncogenes or tumor

suppressors (Esquela-Kerscher and Slack, 2006; Hammond, 2007). Importantly, an miRNA expression profile of human tumors has emerged that is characterized by a defect in miRNA production and global miRNA downregulation (Lu et al., 2005; Calin and Croce, 2006; Gaur et al., 2007). Recent studies have provided possible mechanisms that could explain this miRNA deregulation in cancer: failure of miRNA posttranscriptional regulation (Thomson et al., 2006), CpG island promoter hypermethylation-associated transcriptional silencing (Saito et al., 2006; Lujambio et al., 2007), transcriptional repression by oncogenic factors (Chang et al., 2008), and mutational impairment of

Significance

MicroRNAs (miRNAs) are small noncoding RNAs that regulate gene expression by inhibiting target messenger RNA (mRNA). Data from numerous studies indicate that miRNAs play a critical role in tumorigenesis. The production of mature miRNAs is accomplished via an enzymatic pathway that can go awry at various steps. These defects can explain the reported downregulation of miRNAs in human cancer. Herein, we show that a subset of tumors from the colon, stomach, and endometrium harbor inactivating mutations of *XPO5*, a gene critical to the export of the immature precursor miRNAs (pre-miRNAs) from the nucleus to the cytosol. The re-expression of the wild-type protein rescues the aberrant phenotype and has tumor-suppressor properties. This last finding might also have therapeutic applications.

the *TARBP2* miRNA processing gene (Melo et al., 2009). This last finding is particularly relevant because if the factors involved in miRNA processing pathways are themselves targets of genetic disruption, they might represent another class of tumor-suppressor genes. In this regard, there is an enhancement of tumorigenesis upon depletion of *DICER1* in human cells (Kumar et al., 2007) and heterozygous deletion of *DICER1* in mice (Kumar et al., 2007, 2009; Lambertz et al., 2010). Moreover, reduced *DICER1* expression occurs in lung and ovarian tumors (Karube et al., 2005; Merritt et al., 2008). Under these circumstances, *DICER1* might be described as a haploinsufficient tumor-suppressor gene that is heterozygously deleted in cancer (Kumar et al., 2009). Most importantly, Hill et al. (2009) have identified *DICER1* germline mutations in an inherited cancer syndrome, familial pleuropulmonary blastoma.

The biogenesis of miRNAs in mammalian cells involves both nuclear and cytoplasmic processing (Lee et al., 2002) catalyzed by ribonuclease III (RNase III)-like endonucleases that recognize double-stranded RNAs. miRNAs are initially transcribed as long RNAs, termed primary miRNAs (pri-miRNAs), that contain the mature miRNA as one arm of an RNA stem-loop (Lee et al., 2002). This stem-loop is excised by the nuclear RNase III enzyme DROSHA to give an ~65 nt RNA hairpin, bearing a 2 nt 3' overhang, termed a precursor-miRNA (pre-miRNA) (Zeng and Cullen, 2004). The pre-miRNAs generated in the nucleus require further processing in the cytoplasm, and so the nucleocytoplasmic transport of pre-miRNAs is essential for the maturation process of the miRNAs (Yi et al., 2003; Bohnsack et al., 2004; Kim, 2004; Lund et al., 2004).

One of the key elements in the nuclear export of pre-miRNAs is Exportin-5 (*XPO5*) (Lund et al., 2004). *XPO5* is a member of the karyopherin β family related to human export receptor CRM1 that uses the GTPase Ran to control cargo association (Smith et al., 2002; Bohnsack et al., 2004). Nuclear export of pre-miRNAs is tightly regulated in normal cells and its disruption would also cause the observed phenotype of global downregulation of mature microRNAs in cancer cells. Strikingly, a recent report has demonstrated that some pre-miRNAs are retained in the nucleus of several cancer cell lines (Lee et al., 2008), reinforcing the hypothesis that genetic defects in the pre-miRNA nuclear export genes might occur in human tumors.

Here, we investigated whether genes involved in the export of the pre-miRNAs, such as *XPO5*, undergo loss-of-function mutations in human tumors and the functional significance of such inactivation in nucleocytoplasmic pre-miRNA shuttling and cellular transformation.

RESULTS

Detection of an *XPO5*-Inactivating Mutation in Human Cancer Cells

In order to explore the existence of inactivating mutations in the process of nucleocytoplasmic export of pre-miRNAs, we decided to consider tumors that exhibit microsatellite instability, in the contexts of hereditary nonpolyposis colon cancer (HNPCC) associated with germline mutations in the mismatch repair genes and of sporadic cancers associated with *hMLH1* inactivation by promoter CpG island methylation. Tumors with microsatellite instability progress along a genetic pathway with

a high rate of insertion and deletion mutations in mononucleotide repeats, which often results in the generation of premature stop codons. Illustrative target genes include the growth control gene *TGFBR2* (Markowitz et al., 1995) and the proapoptotic gene *BAX* (Rampino et al., 1997).

We first screened six colorectal (Co115, RKO, SW48, LoVo, HCT-15, DLD-1, and HCT-116), four endometrial (SKUT-1, SKUT-1B, AN3CA, and HEC1B), and two gastric (SNU-1 and SNU-638) cancer cell lines with microsatellite instability for the presence of mutations in all the exonic mononucleotide repeats present in the coding sequences of the two main genes involved in the export of the pre-miRNAs from the nucleus: exportin 5 (*XPO5*) and Ras-related nuclear protein (*RAN*). We detected only wild-type sequences for *RAN* (Figure S1) but found a frameshift mutation in *XPO5*: the insertion of an "A" in an (A)₇ coding microsatellite repeat of exon 32 (position 3546 bp) in the colorectal cancer cell lines HCT-15 and DLD-1 (Figure 1A). The insertion generates a premature termination codon at position 3582 bp. The protein originated from the mutated transcript has altered amino acids 1181–1192 and truncated amino acids 1193–1205. The mutation was present in 24 of 48 (50%) and 25 of 48 (52%) single clone sequences obtained from genomic DNA for HCT-15 and DLD-1, respectively. The same proportion of mutant alleles was found when we used cDNA as the starting material, which indicates that they are heterozygous mutations. The FISH analysis showed that the two alleles were retained in both cancer cell lines (Figure S1).

The analyses of *XPO5* expression by western blot in the total protein extracts from mutant cell lines HCT-15 and DLD-1 demonstrated the presence of the truncated form of the *XPO5* protein (Figure 1B; Figure S1) in addition to the wild-type form. The mutated *XPO5* protein was not present in the wild-type cell lines SW48, HCT-116, and RKO. Most interestingly, when we analyzed nuclear and cytoplasmic fractions separately for *XPO5* protein by western blot in the three *XPO5*-proficient cells (RKO, HCT-116, and SW48) and two *XPO5* mutated cells (HCT-15 and DLD-1), we found that the truncated form of the *XPO5* protein was exclusively present in the nuclear fraction of HCT-15 and DLD-1 cell lines (Figure 1B). To reinforce the protein localization results obtained by western blot, we carried out immunocytochemistry for the *XPO5* protein and observed that in mutated cells (HCT-15 and DLD-1) the *XPO5* protein mainly accumulated in the nucleus (Figure 1B). *XPO5* wild-type cells (HCT-116 and RKO) show *XPO5* staining that spreads equally throughout the nucleus and the cytoplasm (Figure 1B).

The *XPO5* Mutation Traps Precursor microRNAs in the Nucleus, Decreases Processing Efficiency, and Diminishes Target Inhibition by miRNAs

Once the presence of an *XPO5* mutation associated with abnormal protein localization in cancer cells had been confirmed, it became very important to establish, whether the subcellular distribution of pre-miRNAs was affected as well as their processing efficiency, the amount of pre-miRNA that is transformed in its mature form (Experimental Procedures). We first assessed pre-miRNA cellular localization by the study of 24 pre-miRNAs analyzed by qRT-PCR (Schmittgen et al., 2004) in isolated nuclear and cytoplasmic fractions. For all the studied pre-miRNAs, we observed a nuclear accumulation of these

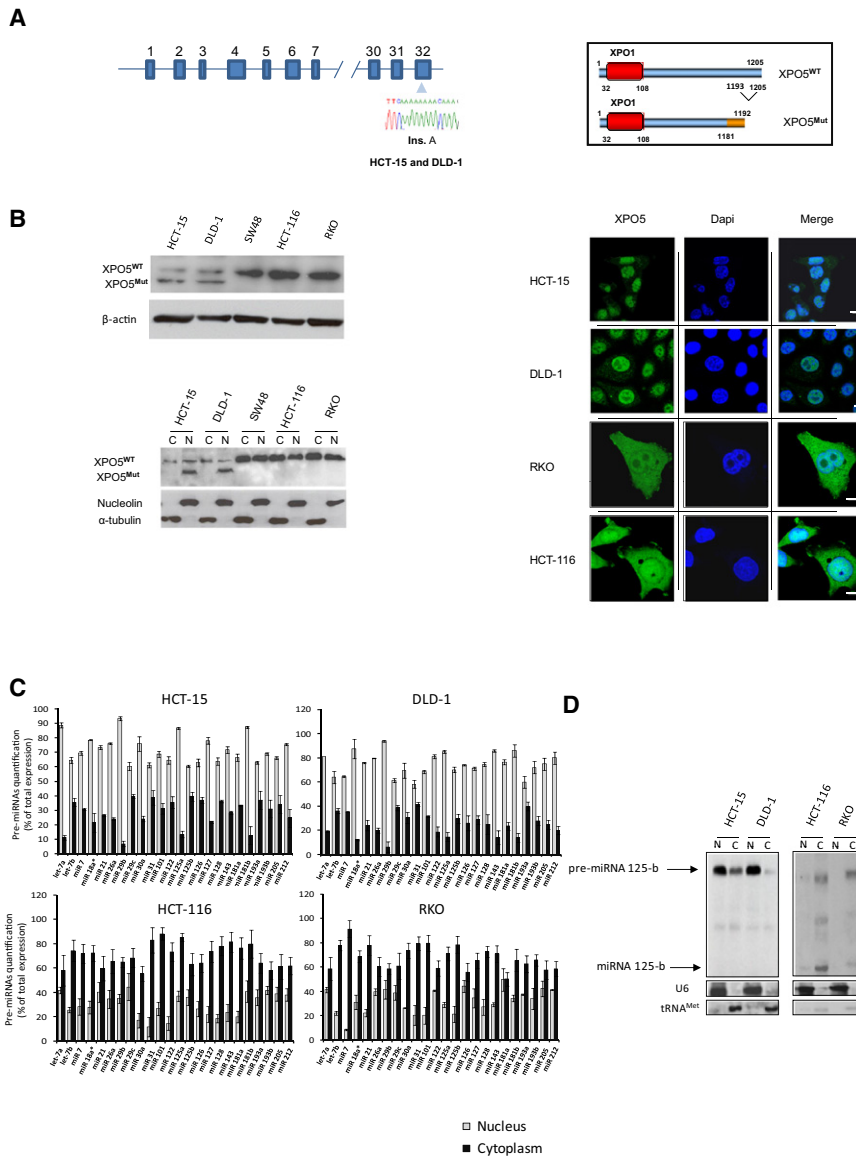


Figure 1. A Mutant XPO5 in Human Cancer

(A) Diagram of the XPO5 gene, with the location of the (A)₇ repeat. Schematic representation of the XPO5 wild-type protein, and the mutated form of XPO5 (the insertion of an "A" in the A₇ repeat alters the open reading frame changing amino acids 1181–1192 and truncating the last 13 amino acids of the protein—amino acids 1193–1205).

(B) XPO5 protein expression analyzed by western blot and immunocytochemistry. XPO5 protein expression using total protein extracts and nuclear (N) versus cytoplasmic (C) fractionated extracts are shown. Only in cell lines harboring the XPO5 mutation was the truncated XPO5 form located exclusively in the nuclear fraction. Immunocytochemistry shows mainly nuclear XPO5^{Mut} protein localization in mutant cells (HCT-15 and DLD-1), while in XPO5 wild-type cells (RKO and HCT-116) the protein was seen to spread throughout the nucleus and cytoplasm. Scale bars, 10 μm.

(C) Higher nuclear levels of 24 precursor miRNAs relative to cytoplasm, quantified by qRT-PCR, are observed in mutant XPO5 cell lines. In the wild-type cell lines (RKO and HCT-116), the highest levels of precursor miRNAs are found in the cytosol. Data shown represent mean ± SD, n = 3.

(D) Northern blot analysis confirmed the accumulation of pre-miRNA 125-b in the nucleus of XPO5 mutant cells (HCT-15 and DLD-1) in sharp contrast to XPO5 wild-type cells (RKO and HCT-116) where it was mainly located in the cytoplasm. U6 and tRNA^{Met} were used as nuclear and cytoplasmic loading control, respectively.

See also Figure S1.

fact, XPOT and XPO5 bind quite complementary sets of tRNAs (Bohnsack et al., 2002).

To strengthen the evidence of a link between XPO5 mutation and the impaired protein shuttling between nucleus and cytoplasm and the defective processing of pre-miRNAs observed, we reconstituted XPO5 function in XPO5 mutant

molecules in XPO5 mutant cells (HCT-15 and DLD-1) (Figure 1C), while in XPO5 wild-type cells (RKO and HCT-116) the pre-miRNAs were found mainly in the cytoplasmic fraction (Figure 1C). Northern blot analysis for miRNA-125-b confirmed its inefficient pre-miRNA processing in XPO5 mutant versus wild-type cells (Figure 1D). Furthermore, we observed that XPO5 mutant cells featured an overall reduction in the efficiency of processing each of the 24 pre-miRNAs molecules, defined as the ratio of mature to precursor miRNA determined by qRT-PCR, relative to XPO5 wild-type cells (Figure S1). Interestingly, XPO5 might also be an auxiliary exporter of transfer RNAs (tRNAs) (Bohnsack et al., 2002; Calado et al., 2002), in parallel to the principal tRNA exporter Exportin-T (XPOT) (Köhler and Hurt, 2007). We did not observe an accumulation of tRNA^{Met} assessed by northern blot in XPO5 mutant cells (HCT-15 and DLD-1) in comparison to wild-type cells (RKO and HCT-116) (Figure 1D). However, this observation does not rule out that other tRNAs are affected. In

cancer cells (HCT-15) (Figure S2). XPO5 levels in the ectopically expressing cells in comparison to the endogenous levels in the sham/control transfected cells are shown in Figure S2. Transfection of an N-terminal flag-tagged wild-type form of XPO5 protein (XPO5^{WT}) in HCT-15 cells showed that the wild-type transfected protein localizes in the nucleus and cytoplasm (Figure 2A). However, the transfection of a N-terminal flag-tagged construct carrying the described XPO5 mutation (XPO5^{Mut}) in HCT-15 cells shows an XPO5 protein that it is located inside the nucleus and no signal is seen in the cytoplasm (Figure 2A). Wild-type endogenous XPO5 localization was unaffected upon mock transfection (Figure S2). Because the approach described looks at proteins steady-state levels, we also formally proved that FLAG-XPO5^{Mut} is trapped in the nucleus using the heterokaryon approach (Lee et al., 1996). Heterokaryon assays demonstrated that XPO5^{Mut} is not capable of shuttling between the nucleus and the cytoplasm of the empty-vector and XPO5^{Mut} N-terminal flag

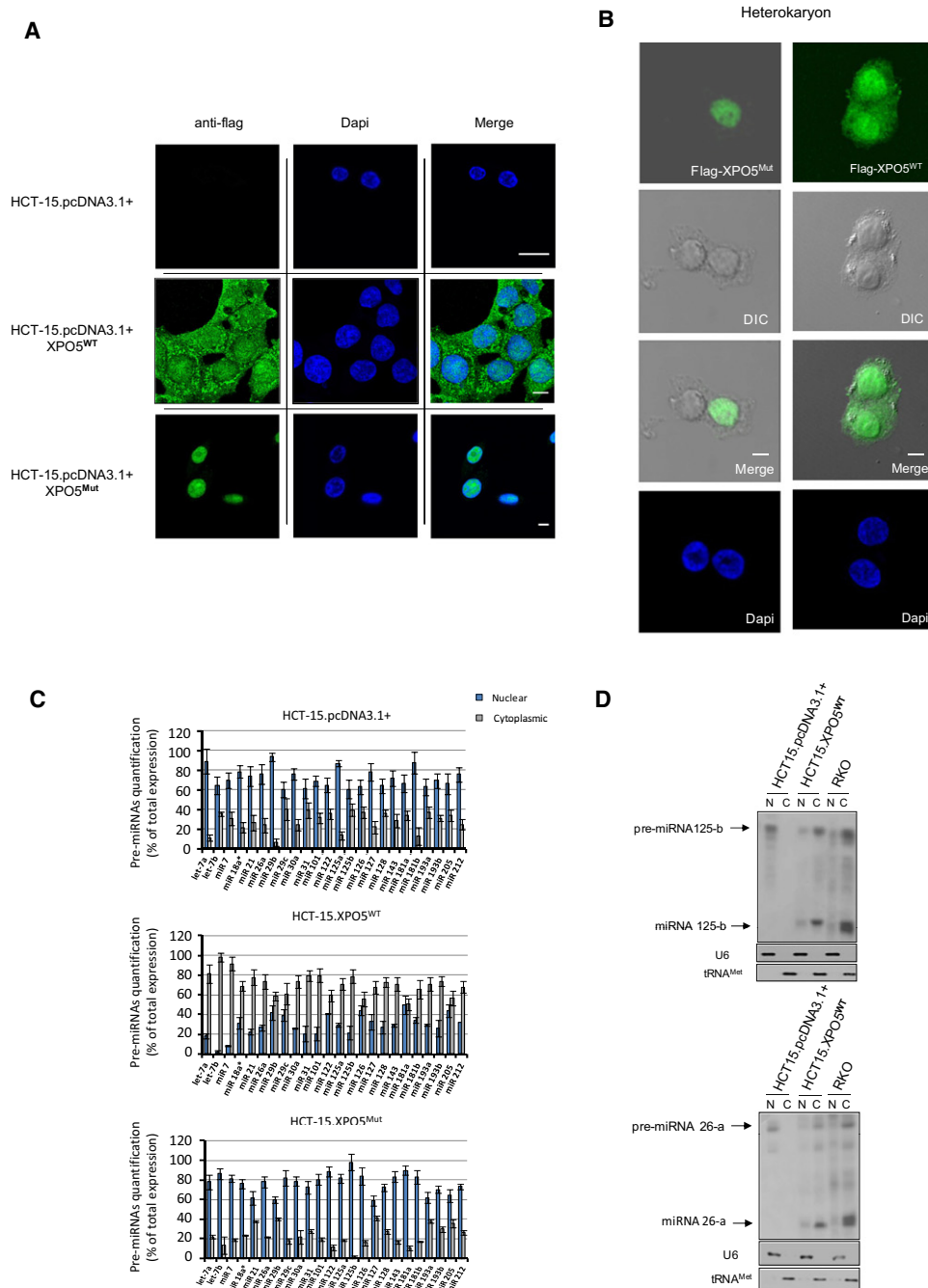


Figure 2. Transfection of Wild-Type XPO5 Rescues Pre-miRNA Location

(A) XPO5 protein expression was restored after transfecting flagged XPO5 wild-type in HCT-15 cell line. As a control, XPO5 mutant form was also stably transfected in HCT-15. Transfected proteins were detected by immunocytochemistry using an anti-flag antibody. XPO5 mutant form presented exclusively nuclear accumulation by immunocytochemistry. Scale bars, 10 μ m.

(B) Heterokaryon assay shows nuclear retention of XPO5^{Mut} protein transfected in HCT-116 cell line (left panel). Positive control for the heterokaryon assay using wild-type XPO5 is shown in the right panel. DIC, differential interference contrast. Scale bars, 10 μ m.

(C) HCT-15 cell line transfected with XPO5^{WT} showed a displacement of the described 24 pre-miRNAs from the nucleus to the cytoplasm while no alteration of the pre-miRNAs localization was seen in XPO5^{Mut}-transfected HCT-15 cells. Data shown represent mean \pm SD, n = 3.

(D) Northern blot analysis confirmed the cytoplasmic enrichment of pre-miR-125-b and pre-miR-26-a in XPO5^{WT} HCT-15-restored cells. U6 and tRNA^{Met} were used as nuclear and cytoplasmic loading control, respectively.

See also Figure S2.

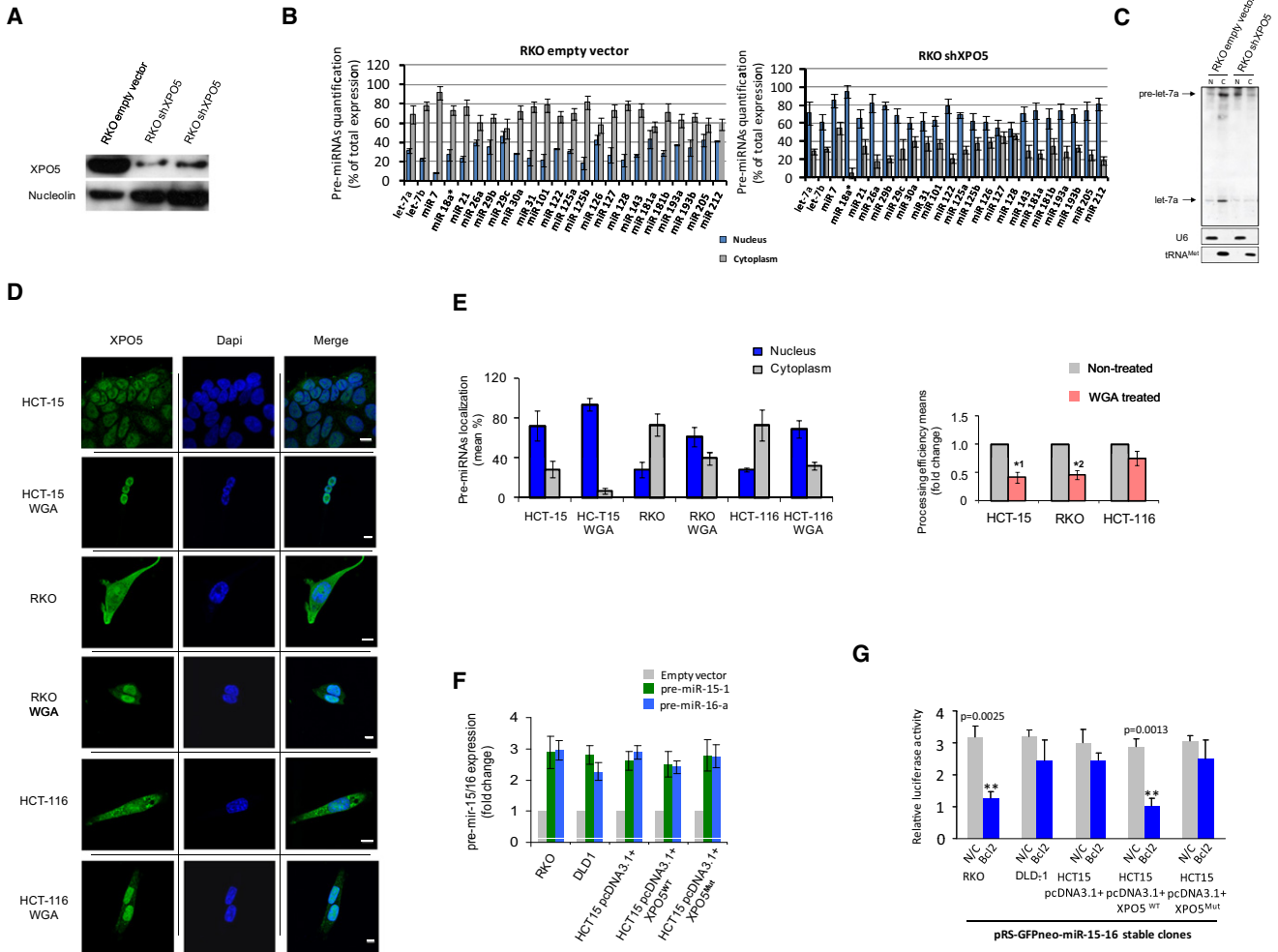


Figure 3. XPO5 Stable Downregulation and Pharmaceutical Inhibition Mimics the Phenotype of XPO5 Impaired Cells

(A) Protein blot showing stable downregulation of XPO5 protein expression in XPO5-proficient RKO cell line using short-hairpin approach. (B) XPO5-downregulated RKO cells showed an increased concentration of 24 pre-miRNAs in the nucleus compared with empty vector transfected cells determined by qRT-PCR. (C) Northern blot analysis confirmed the nuclear enrichment of pre-let-7a in XPO5 RKO downregulated cells. U6 and tRNA^{Met} were used as nuclear and cytoplasmic loading control, respectively. (D) XPO5 is retained in the nuclear fraction upon delivery of WGA by electroporation. Scale bars, 10 μm. (E) The inhibition of nuclear export by WGA treatment retains pre-miRNAs in the nuclear fraction of XPO5 wild-type and impairs pre-miRNA processing efficiency (*¹ p = 0.0031, *² p = 0.0042). (F) Expression level of pre-miRNAs 15-1 and 16-a in stably transfected cells measured by qRT-PCR analysis. (G) Transient transfection of 3'UTR of Bcl2 under a luciferase reporter in pRS-GFPneo-miR-15-16 stable clones. Only XPO5^{WT}-restored cell lines, together with RKO XPO5-proficient cell lines, showed significantly lower luciferase activity. NC: control using mutated nonfunctional Bcl2 3'UTR. pGL2 basic vector was used as an empty vector control. One microgram total DNA vector per transfection was used to normalize the diagram. Data shown represent mean ± SD, n = 3. See also Figure S3.

transfected HCT-116 fused cells (Figure 2B). Most importantly, XPO5 mutant cells transfected with the wild-type protein underwent a relocation of pre-miRNAs from the nucleus to the cytosol (Figure 2C). Northern blot analyses for miRNA-125-b and miRNA-26-a confirmed the described results (Figure 2D). XPO5 wild-type transfection was associated with an increased processing capacity for the 24 pre-miRNAs determined by qRT-PCR (Figure S2). Transfection of the mutant form of XPO5 in HCT-15 cells was unable to rescue the phenotype: pre-miRNAs were essentially located in the nucleus (Figure 2C) and no increase in pre-miRNA processing efficiency was observed (Figure S2),

implying the loss of function features of the identified mutation. Using primers specific for the 30 pri-miRNAs that originate the studied 24 pre-miRNAs (details in Experimental Procedures), we have observed that pri-miRNA levels did not change upon transfection of the wild-type or mutant XPO5, supporting that the mutation only affects pre-miRNAs (). tRNA^{Met} (Figure 2D) levels were also unchanged upon transfection of the wild-type or mutant XPO5.

In sharp contrast, the stable downregulation of XPO5 by independent transfection of three different short-hairpins that targets XPO5 in cells with wild-type XPO5 (RKO) (Figure 3A; Figure S3)

was associated with enhanced retention of the studied 24 pre-miRNAs inside the nucleus (Figure 3B; Figure S3). Northern blot for miRNA let-7a confirmed the described results (Figure 3C). An impairment of pre-miRNA processing efficiency was also observed upon XPO5 depletion (Figure S3). siRNA against the mutant XPO5 transcript in HCT-15 and DLD-1 cells did not cause any evident effect in pre-miRNA processing capacity (Figure S3). Pri-miRNAs (Figure S3) and tRNA^{Met} (Figure 3C) levels were unchanged upon XPO5 depletion. Furthermore, we were able to mimic the mutant XPO5 phenotype using wheat germ agglutinin (WGA). WGA blocks nuclear pore complexes by binding to GlcNAc-modified nucleoporins (Mohr et al., 2009). Using electroporation to deliver WGA into the cells (Todorova, 2009), we observed that XPO5 wild-type cells (RKO and HCT-116) underwent confinement of the XPO5 protein in the nucleus (Figure 3D), nuclear accumulation of pre-miRNAs (Figure 3E, left graph), and decreased pre-miRNA processing efficiency (Figure 3E, right graph) that closely resemble the phenotype observed in XPO5 mutant cells.

We also wondered whether the impaired nuclear export associated with XPO5 mutation had an impact on the inhibitory efficiency of miRNA target genes. To address this issue, we stably transfected wild-type, mutant and reconstituted XPO5 cells with pRS-GFPneo-miR-15-16, a vector that produces a pre-miRNA that needs to be nuclear exported in order to be processed correctly and give rise to its mature forms (miR-15-a and miR-16-1) (Figure 3F). To show interaction of the mature miRNAs with its target 3'UTR, we transiently transfected to the described cells the 3'UTR of the oncogene Bcl2 under a luciferase reporter, a known and validated target of miR-15-a/16-1 (Calin et al., 2008). We observed that luciferase activity was significantly decreased only in XPO5 wild-type (RKO) and XPO5^{WT}-restored (HCT-15) colorectal cancer cells. No significant effect was demonstrated in XPO5 mutant cells such as DLD-1 and HCT-15 (Figure 3G). Most importantly, luciferase activity was also unaffected in HCT-15 cells transfected with the mutant form of XPO5 (XPO5^{Mut}) (Figure 3G). Consistent with these data, we also observed that, following stable EGFP transfection in XPO5^{WT} and XPO5^{Mut}-HCT-15 cells (Figure S3), a short-hairpin against EGFP was only able to achieve complete silencing in XPO5^{WT}-restored cells (Figure S3). qRT-PCR on EGFP mRNA was used as a quantitative measure of the shRNA efficiency (Figure S3).

XPO5 Mutant Form (XPO5^{Mut}) and the Functional Impairment of the Pre-miRNA/XPO5/Ran-GTP Complex

Once we had demonstrated that XPO5 mutant cells had a defect with respect to exporting pre-miRNAs out of the nucleus and consequently an impaired processing efficiency, we sought to determine why the mutant form of the XPO5 protein is trapped inside the nucleus. It is well documented that pre-miRNAs are specifically bound by XPO5, acting in concert with the GTP-bound form of the Ran cofactor (Bohnsack et al., 2004; Lund et al., 2004; Yi et al., 2003). Since cargo binding to XPO5 is promoted by Ran-GTP, we decided first to establish whether Ran could bind the XPO5^{Mut} form. We performed GST pull-down experiments with recombinant proteins purified from *Escherichia coli* in the absence or presence of the cargo, the pre-miRNA molecule pre-let-7a. First, as expected, we observed that the addition of pre-let-7a increased the affinity of the poly-

histidine-tagged XPO5^{WT} to bind GST-Ran in a GTP-dependent manner (Figure 4A, lanes 1 and 2). However, the polyhistidine-tagged XPO5 mutant form, although also able to bind to GST-Ran in a GTP-dependent manner, did not show any cooperativity for Ran binding in the presence of cargo (pre-let-7a) (Figure 4A, lanes 3 and 4). As a negative control, we used a construct lacking 108 amino acids at the N-terminal domain of XPO5 (XPO5^{Δ108}) that is responsible for Ran-GTP coupling (Brownawell and Macara, 2002) (Figure 4A, lanes 5 and 6). Our findings are in agreement with previous observations that described Ran/GTP coupled to the N-terminal of XPO5 protein (Brownawell and Macara, 2002). This domain is not altered in the XPO5^{Mut} form that we describe herein. Knowing that a ternary complex of pre-miRNA/XPO5/Ran-GTP is necessary for efficient nuclear export (Zeng and Cullen, 2004), we decided to analyze the capacity of XPO5^{WT} and XPO5^{Mut} forms to bind pre-miRNAs molecules using the pre-miRNA molecule pre-let-7a.

We transfected a 3'-biotin labeled synthetic pre-let-7a in XPO5 mutant HCT-15 cells stably transfected with the empty vector (pcDNA3.1+), the FLAG-XPO5 wild-type (FLAG-XPO5^{WT}) and the FLAG-XPO5 mutant (FLAG-XPO5^{Mut}) forms, followed by FLAG-XPO5 protein and pre-let-7a cellular localization by immunodetection of Flag and biotin, respectively. In empty vector transfected cells, we observed that pre-let-7a is maintained within the nucleus after transfection during a 2 hr period (Figure 4B, left panels and left graph). In HCT-15 cells with reconstituted XPO5 activity (FLAG-XPO5^{WT}), however, we observed efficient export of the labeled pre-let-7a into the cytoplasm 1 hr after transfection and disappearance of the biotin signal in the cytoplasm 2 hr after transfection (Figure 4B). Furthermore, XPO5^{WT} flag-tagged protein was found in the same cellular compartment with pre-let-7a throughout the 2 hr after transfection translocating from the nucleus to the cytoplasm 1 hr after transfection (Figure 4B). The same results for XPO5 wild-type context had been reported for pre-miR-31 export (Bohnsack et al., 2004). When the same assay was developed on HCT-15 FLAG-XPO5^{Mut} transfected cells, pre-let-7a was not efficiently transported into the cytoplasm, and 2 hr after transfection there was still biotin labeling inside the nucleus (Figure 4B). Results of pre-let-7a levels obtained by qPCR of fractionated nuclear and cytoplasmic samples confirmed the immunocytochemistry data (Figure 4C). Furthermore, XPO5^{Mut} flag-tagged protein showed no translocation to the cytoplasm but stayed in the nucleus for the 2 hr period (Figure 4B, right panel anti-flag labeling). As a control for the transfection procedure, the staining for the XPO5 endogenous protein demonstrated that its main nuclear localization in the HCT-15 mutant cells was unchanged right before and immediately after pre-let-7a transfection (Figure S4).

Once the impairment of pre-let-7a export mediated by a defective XPO5 protein had been demonstrated, we tested the capacity of the XPO5 mutant form to bind pre-let-7a in a Ran-GTP-dependent manner. For this purpose, we used the 3' biotin-labeled synthetic pre-let-7a to incubate with purified, recombinant His-tagged human XPO5^{WT}, XPO5^{Mut}, and recombinant Ran in the presence of GTP. We determined by gel shift analysis that the biotin labeled pre-let-7a did not bind XPO5^{Mut} in the presence of Ran and GTP (Figure 4D). However, pre-let-7a formed a readily detectable complex when incubated with XPO5^{WT} (Figure 4D). To reinforce the specificity of the

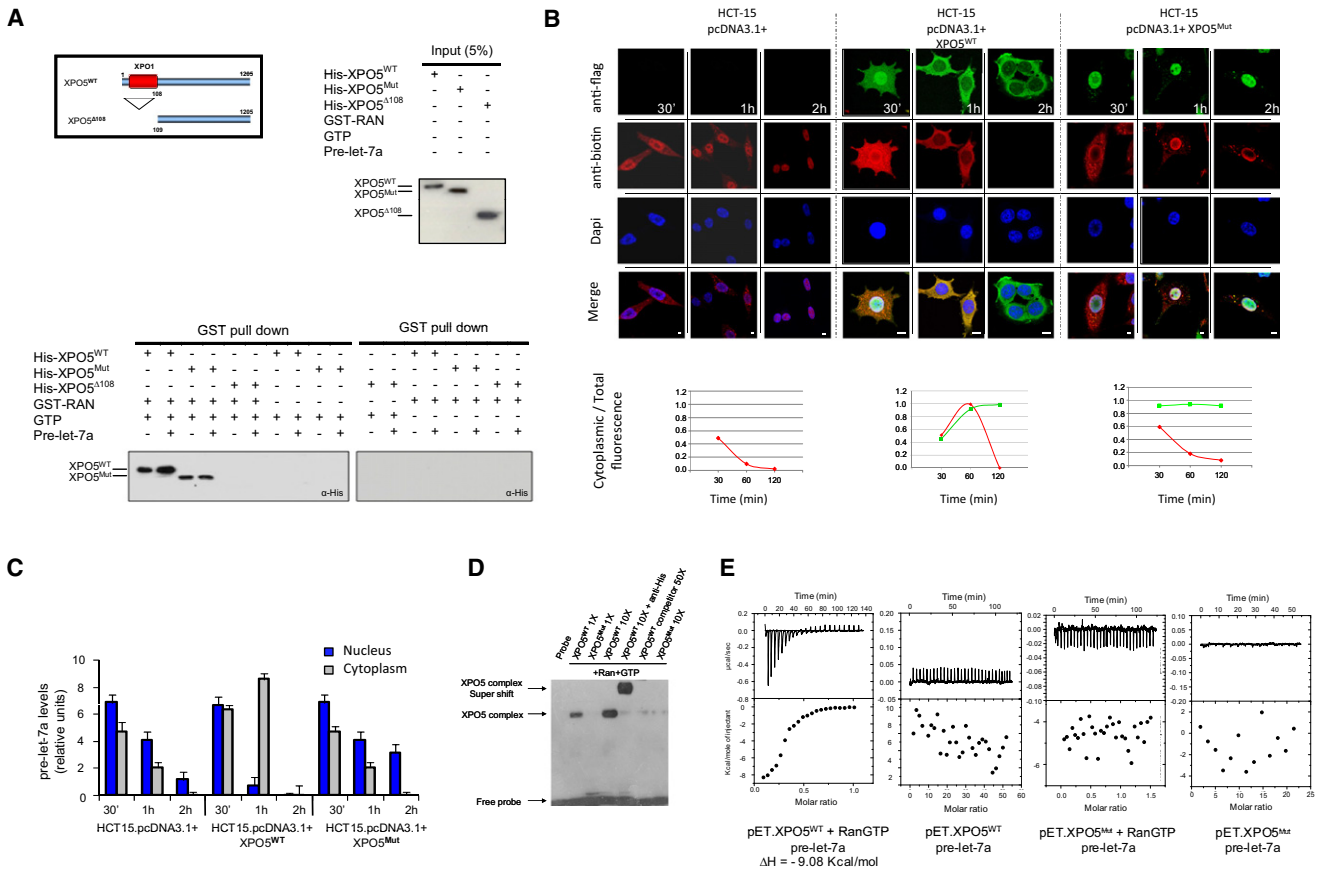


Figure 4. XPO5 Mutant and the Functional Impairment of the Pre-miRNA/XPO5/Ran-GTP Complex

(A) GST-Ran fusion protein was incubated with His-XPO5^{WT} and His-XPO5^{Mut} in the presence of GTP and in the absence or presence of the cargo, the pre-miRNA molecule pre-let-7a. Both wild-type and mutant forms of XPO5 were able to bind to Ran in a GTP-dependent manner (lanes 1, 2 and 3, 4, respectively). As a negative control we used a cloned XPO5 protein lacking the first 108 amino acids (N-terminal) responsible for binding to Ran (XPO5^{A108}, lanes 5 and 6). The addition of pre-let-7a (lane 2 versus lane 1) increased the affinity of XPO5^{WT} to bind GST-Ran in a GTP-dependent manner. The XPO5 mutant form did not show any cooperativity for Ran binding in the presence of cargo (pre-let-7a) (lane 4 versus lane 3).

(B) 3' Biotin-labeled pre-let-7a molecule was transfected in empty vector, XPO5^{WT} and XPO5^{Mut} HCT-15 stable transfected cell lines. Upon transfection, and during a 2 hr period, pre-let-7a and FLAG-XPO5^{WT} or FLAG-XPO5^{Mut} proteins were followed by immunocytochemistry using anti-biotin and anti-flag staining, respectively. The graphs on the bottom illustrate the quantification of fluorescence signal in the cytoplasm over time. Only in XPO5^{WT} HCT-15 restored cell line there is an increase in cytoplasmic signal 1 hr after transfection due to pre-let-7a[Biotin] nuclear export. Scale bars, 10 μm.

(C) qRT-PCR of pre-let-7a. Only in XPO5^{WT} HCT-15 restored cell line there is a pre-let-7a displacement from the nucleus to the cytoplasm at 1 hr posttransfection. Data shown represent mean ± SD, n = 3.

(D) Gel shift assays were performed with pre-let-7a probe, 3' biotin-labeled, and 3 μM of each recombinant XPO5^{WT} and XPO5^{Mut} in the presence of Ran protein and GTP. The specific RNA-protein complexes are indicated by arrows. Only XPO5^{WT} is able to bind pre-let-7a specifically. A supershift signal is seen when anti-His antibody is added to the reaction when using XPO5^{WT}. XPO5^{Mut} form is not able to bind pre-let-7a.

(E) Isothermal titration calorimetry data for XPO5^{WT} and XPO5^{Mut} with pre-let-7a in the presence or absence of RanGTP. The upper panels show the calorimetric titrations for 10 μl injections with 240 s time lapses. The lower panels represent the integrated heat values as a function of the protein/pre-miRNA molar ratio in the calorimetric cell. An exothermic reaction ($\Delta H = -9.08$ Kcal/mol) is perceived between XPO5^{WT} protein and pre-let-7a in the presence of RanGTP while no reaction takes place between XPO5^{Mut} and pre-let-7a. Both XPO5^{WT} and XPO5^{Mut} fail to bind pre-let-7a in the absence of RanGTP. See also Figure S4.

formed RNA-protein complex, we wondered whether unlabeled competitor RNA would block complex formation if added in excess, and whether a supershift could be observed when the antihistidine antibody was added to the reaction. Formation of the pre-let-7a/XPO5/Ran-GTP complex was indeed inhibited when the unlabeled competitor RNA was used and a supershift was observed when antihistidine antibody was added to the reaction (Figure 4D). Most importantly, the same binding results were obtained by calorimetric assays (Figure 4E). The precursor let-7a molecule reacts exothermally ($\Delta H = -9.08$ Kcal/mol)

with XPO5^{WT} protein in the presence of Ran-GTP, while no reaction was observed between the XPO5^{Mut} form and the precursor miRNA molecule (Figure 4E). The XPO5^{WT} and XPO5^{Mut} proteins did not bind pre-let-7a in the absence of Ran-GTP (Figure 4E). We also analyzed if the mutant XPO5 protein was in any way able to interfere in the binding of the wild-type XPO5 protein to its pre-miRNA substrates. Using both EMSA and calorimetric studies to assess the binding of the wild-type XPO5 protein to pre-let-7a in the presence of the XPO5 mutant protein and Ran-GTP, we observed that the binding to the pre-miRNA

substrate was not affected by the presence of the XPO5 mutant protein (Figure S4).

Overall, these results suggest that a region in the C-terminal of XPO5 protein is involved in the binding and/or recognition of pre-miRNAs as a cargo substrate. In XPO5 mutant cells, such as HCT-15 and DLD-1, the protein is not able to load the precursor miRNA molecule, the pre-miRNA/XPO5/Ran-GTP ternary complex cannot be assembled and pre-miRNAs accumulate in the nucleus.

Tumor-Suppressor Features of the XPO5 Protein

Once we had demonstrated how the described XPO5 mutation in cancer cells impaired the export of pre-miRNAs, we wished to determine its contribution to the tumorigenic phenotype. Thus, we took a triple approach to show how XPO5 genetic disruption causes a defect in the expression of mature miRNAs with tumor-suppressor features, how its restoration leads to cancer growth inhibition both in vitro and in vivo, and how XPO5 mutations are present in human primary tumors.

We first analyzed the miRNA expression profile of wild-type (RKO and HCT-116), mutant (HCT-15 and DLD-1), reconstituted (HCT-15 and DLD-1 XPO5^{WT}), and mutant transfected (HCT-15 and DLD-1 XPO5^{Mut}) XPO5 cell lines using a comprehensive expression miRNA microarray platform that covers 731 miRNAs (Calin et al., 2007). Among these, the expression of around 50% miRNAs was initially absent in the colorectal cancer cell lines RKO (n = 449), HCT-116 (n = 448), DLD-1 (n = 421), and HCT-15 (n = 398). We used Class Comparison ($p < 0.001$) to identify the miRNAs differentially expressed between classes, and Class Prediction ($p < 0.001$, repeated 100 times, K-fold cross-validation method, where $K = 10$) to identify patterns of miRNAs that can discriminate groups of samples. The two XPO5 mutant cell lines were characterized as having a significant downregulation of 85 miRNAs compared with the two wild-type XPO5 cell lines (Figure 5A). Most importantly, the reintroduction of XPO5 in the mutant cells upregulated 114 miRNAs (Figure 5A, HeatMap) that included 80 of 85 (94%) of the described miRNAs. qRT-PCR was used to validate the microarray data for 11 miRNAs (six miRNAs upregulated in XPO5^{WT}-transfected cells and five miRNAs with similar levels) (Figure 5B). We did not observe any shift in the miRNA expression profile when the XPO5 mutant cells were transfected with the XPO5^{Mut} form. Strikingly, for these 80 miRNAs downregulated in XPO5 mutant cells and whose expression is restored in reconstituted cells, 76.8% have potential tumor-suppressor features (Figure 5C; Medina and Slack, 2008; Spizzo et al., 2009). Most importantly, this impairment of tumor-suppressor miRNAs in XPO5 mutant cells is associated with the upregulation of their respective target oncoproteins that is reverted by the transfection of wild-type XPO5, such as we observed for *EZH2* (miR-26a), *MYC* (miR-192, miR-215, let-7, and miR-24), and *K-RAS* (miR-192, miR-215, and let-7) (Figure 5D). One of the best examples was the miR-200 family of tumor-suppressor miRNAs that targets *ZEB1*, a known inhibitor of E-cadherin (CDH1) expression (Burk et al., 2008). The miR-200 family was downregulated in XPO5 mutant cells and, upon XPO5 transfection, we did not only observe upregulation of the miR-200 transcripts, but also downregulation of *ZEB1* and upregulation of its targets E-cadherin, *CRB3*, *INADL*, and *LGL2* (Burk et al., 2008; Figure 5E).

Most notably, the ectopic expression of XPO5 in the mutant cells had cancer growth-inhibitor features (Figure 6). Upon transfection of the wild-type XPO5 in HCT-15 mutant colorectal cancer cells, the cells proved less viable in the MTT assay (Figure 6A) and had a markedly reduced percentage colony formation density (Figure 6B). Transfection of the XPO5^{Mut} form in HCT-15 cells was unable to reduce cell viability (Figure 6A) and had no impact on the colony formation assay (Figure 6B). Overexpression of XPO5 in the wild-type XPO5 colorectal cancer cell line RKO was unable to reduce cell viability (Figure S5), underscoring the specific growth-inhibitory effect of XPO5 only in XPO5 mutant cells. We next tested the ability of XPO5^{WT}-transfected HCT-15 cells to form tumors in nude mice compared with empty vector transfected cells or with the XPO5^{Mut} form (Figure 6C; Figure S5). HCT-15 XPO5 mutant cells transfected with the empty vector or the mutant gene formed tumors rapidly, but cells with wild-type XPO5 expression had much lower tumorigenicity (Figure 6C; Figure S5). In sharp contrast, the stable downregulation of XPO5 by the short hairpin RNA approach in cells with wild-type XPO5 (RKO) was associated with increased cell viability (Figure 6D), increased colony density formation (Figure 6E), and enhanced tumorigenicity in nude mice (Figure 6F; Figure S5). The use of two additional different shRNAs against XPO5 in RKO cells confirmed the observed enhancement of cell viability and colony formation (Figure S5). Most importantly, when we used siRNAs against XPO5 in cancer cells heterozygous for the XPO5 mutation (HCT-15 and DLD-1), we observed that the complete abrogation of XPO5 expression was toxic, according to the XTT and trypan blue assays (Figure S5). These findings are in agreement with the deleterious effects observed upon the full abolishment of other miRNA processing genes such as *DICER1* (Bernstein et al., 2003), where a haploinsufficient tumor-suppressor role has also been proposed (Kumar et al., 2007, 2009; Hill et al., 2009; Lambert et al., 2010). siRNA against the mutant XPO5 transcript in HCT-15 and DLD1 cells did not cause any evident effect in cell viability (Figure S5). Combined siRNAs of wild-type and mutant XPO5 caused a similar cell toxicity in XPO5 mutant cells than the one observed in single siRNA of wild-type XPO5 (Figure S5).

Finally, we sought to measure the frequency of the described XPO5 disruption in human primary tumors. We assessed the XPO5 mutational status of 337 human primary malignancies with microsatellite instability, including colorectal tumors arising in those patients with germline defects in one mismatch repair allele (HNPCC) (n = 38) and apparently sporadic colorectal (n = 211), gastric (n = 58), and endometrial (n = 30) cancers where mismatch repair gene function was somatically inactivated (Table 1). We found that XPO5 frameshift mutations were present in 22.8% (77 of 337) of the primary tumors analyzed. The described insertion of an "A" in the (A)₇ coding microsatellite repeat of exon 32 (Figure 1A) was found in 11.6% (39 of 337) of cases. Interestingly, we discovered two other XPO5 frameshift mutations in primary tumors that we did not observe in any cell line: a deletion of an "A" in the same (A)₇ coding microsatellite repeat of exon 32 and a deletion of an "A" in an (A)₄ repeat of exon 32. These two mutations were present in 30 (8.9%) and 8 (2.4%) cases, respectively. The deletion of an "A" in the (A)₇ repeat changes amino acid composition of the protein from amino acids 1179–1193 and truncates the last 11 amino acids

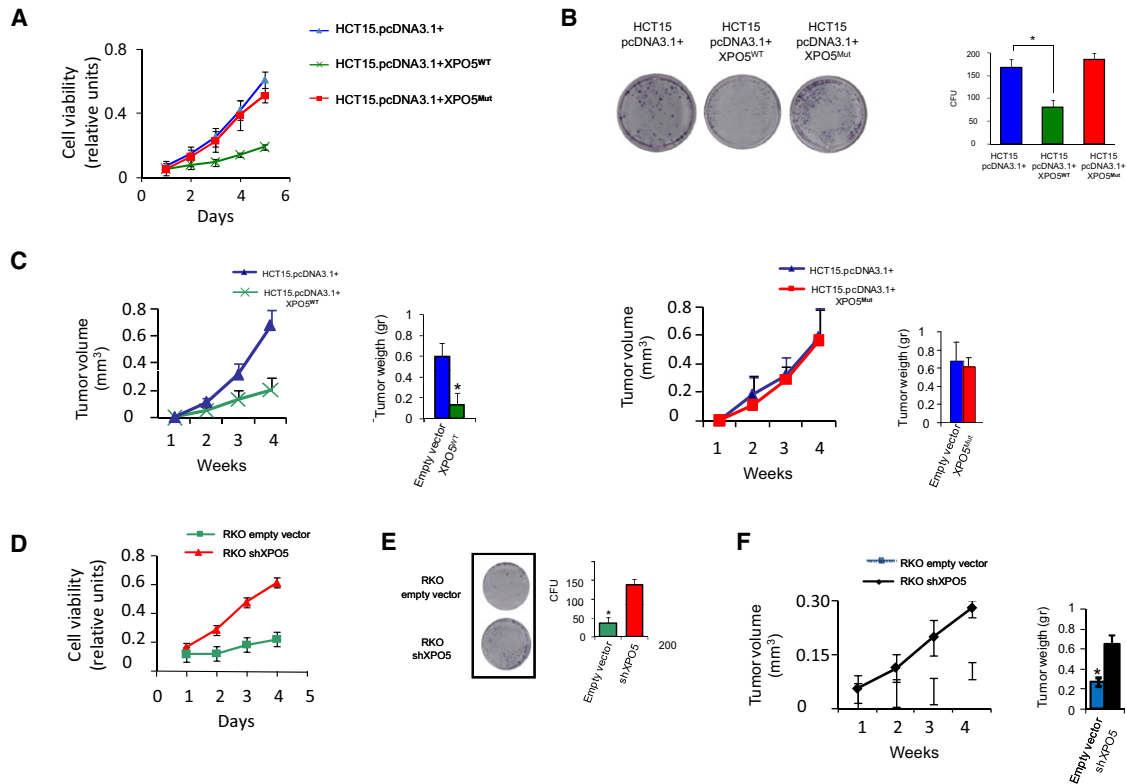


Figure 6. Tumor-Suppressor Features of XPO5^{WT} Protein

(A) The MTT assay showed that mutant XPO5 HCT-15 cells transfected with wild-type XPO5 are less viable than empty vector transfected cells ($p = 0.0015$). Transfection with XPO5^{Mut} did not affect cell viability. Data shown represent mean \pm SD, $n = 3$.
 (B) The colony formation assay showed that mutant XPO5 HCT-15 cells transfected with XPO5^{WT} significantly formed fewer colonies than empty vector transfected cells ($p < 0.001$). Transfection with XPO5^{Mut} did not affect colony formation. Data shown represent mean \pm SD, $n = 3$.
 (C) Effect of XPO5 transfection on the growth of HCT-15 cells in nude mice. Tumor volume was monitored over time and the tumor was excised and weighted at 30 days. There is a significant decrease in tumor volume and weight for the wild-type XPO5 transfected cells (left graphs, $p = 0.008$). Transfection of XPO5^{Mut} did not affect tumor growth of HCT-15 cells injected in nude mice (right graphs, $p = 0.234$). Data shown represent \pm SEM, $n = 10$.
 (D) RKO short-hairpin XPO5 transfected cells showed higher cell viability ($p = 0.0012$). Data shown represent mean \pm SD, $n = 3$.
 (E) Downregulation of XPO5 enhanced colony formation of RKO cells ($p < 0.0001$). Data shown represent mean \pm SD, $n = 3$.
 (F) RKO cells stably downregulated for XPO5 showed enhanced tumorigenic capacity (volume and weight) when injected into nude mice ($p = 0.001$). See also Figure S5.

of XPO5. The deletion of an “A” in the (A)₄ repeat, also present in exon 32, changes the amino acid composition of the protein from amino acids 1167–1205. We have cloned these two XPO5 mutations identified in the primary tumors and developed the corresponding *in vitro* and *in vivo* assays. We have observed that, upon transfection in XPO5 mutant HCT-15 cells, both mutations originate XPO5 proteins that at steady-state levels present nuclear localization, are unable to enhance miRNA processing efficiency, and do not affect cell viability (Figure S6). No single tumor featured more than one mutation, which highlights the functional relevance of each mutational event. Most importantly, none of the 77 tumors with XPO5 mutations had a mutation in *TARBP2*, the miRNA biogenesis gene also found alter in microsatellite unstable neoplasms (Melo et al., 2009), a result that emphasizes the unique role of XPO5 genetic defects in tumorigenesis. No significant differences in XPO5 mutation frequency were found between inherited and sporadic tumors or between tumor types (Table 1). The described XPO5 mutations were not present in primary colorectal tumors without microsatellite insta-

bility (0/42), normal colorectal mucosa (0/50), or in normal lymphocytes from healthy donors (0/80) (Table 1). Thus, XPO5 mutations are common events in microsatellite unstable tumors from the colon, stomach, and endometrium.

DISCUSSION

It is estimated that about 30% of human genes are putative targets of miRNAs; hence, they exert a critical role in numerous biological processes. Thus, it is not surprising that an aberrant miRNA expression profile occurs in a wide range of human diseases. This is particularly true for human cancer, in which the expression of miRNAs is markedly deregulated (Lu et al., 2005; Cummins et al., 2006). Like protein-coding genes, miRNAs can act as tumor suppressors (Hammond, 2007) or oncogenes (Esquela-Kerscher and Slack, 2006). Although the oncogenic role of some particular miRNAs has been clearly demonstrated, increasing evidence supports the concept that global downregulation of mature miRNAs is a common hallmark of human tumors

Table 1. Frequency of XPO5 Mutations in Cancer Cell Lines, Primary Tumors, and Normal Tissues

Sample Type	Cell Lines	Tissue Samples
Colon tumors from HNPCC	—	10/38 (26.3%)
Sporadic colon tumors (MSI+)	2/6 (33.3%)	47/211 (22.3%)
Sporadic gastric tumors (MSI+)	—	16/58 (27.6%)
Sporadic endometrial tumors (MSI+)	0/4	4/30 (13.3%)
Sporadic colon tumors (MSI-)	0/4	0/42
Normal colon	—	0/50
Normal lymphocytes from healthy donors	—	0/80

HNPCC, hereditary nonpolyposis colon cancer; MSI+, tumors with microsatellite instability; MSI-, tumors without microsatellite instability. See also Figure S6.

(Calin and Croce, 2006; Gaur et al., 2007; Lu et al., 2005). Many explanations can be invoked to explain this phenotype, and, herein, we propose another one: genetic defects in the nuclear export machinery of pre-miRNAs. Our description of inactivating mutations in *XPO5*, a key gene in the nuclear export of pre-miRNAs (Yi et al., 2003; Lund et al., 2004), highlights the relevance of an intact export mechanism of miRNA-related molecules to maintain the cellular homeostasis. The relevance of the described genetic alteration in *XPO5* in human cancer is supported by the observation of *XPO5* deletions in different malignancies (Zhang et al., 2008) and the described accumulation of pre-miRNAs in particular cancer cell lines (Lee et al., 2008).

From a functional point of view in normal cells, the *XPO5* protein continuously traverses the nuclear envelope (Brownawell and Macara, 2002), for which reason it should be found in the nuclear and cytoplasmic cellular compartments. However, the described *XPO5* mutations prevent *XPO5* translocation and “sequester” pre-miRNAs in the nucleus, clogging miRNA biogenesis and function. Our data are in agreement with Yi et al. (2003), where the knockdown of *XPO5* caused diminished levels of pre-miR-30 in the cytoplasmic fraction. Others have already defined the pre-miRNA structural requirements for binding to *XPO5* (Zeng and Cullen, 2004). Pre-miRNAs are specifically bound by *XPO5* acting in concert with the GTP-bound form of the Ran cofactor (Bohnsack et al., 2004) and this pre-miRNA/*XPO5*/Ran-GTP ternary complex is recognized by proteins of the nuclear pore complex. The *XPO5* mutant cancer form identified is still able to bind to the Ran protein, but binding cooperativity cargo-Ran has been lost due to the impaired pre-miRNA recognition. Thus, subcellular distribution of *XPO5* protein is dependent, not only on Ran-GTP binding to its N-terminal region (Bohnsack et al., 2004), but also to pre-miRNA binding. Interestingly, Okada et al. (2009) has recently described the crystal structure of the complex formed between *XPO5*/Ran with the pre-miRNA molecule. Remarkably, this structural study only modeled residues 1–1082 of the *XPO5* protein, therefore leaving uncharacterized the residues altered in the *XPO5*^{Mut} form present in cancer, although it was suggested that the C-terminal of *XPO5* was flexible (Okada et al., 2009). It is worth to consider that the

pre-miRNA used to prepare the recombinant complex for crystallization was much shorter than the one used in our study, which contains the stem loop and resembles the physiological pre-miRNA molecule that is exported out of the nucleus. Therefore, it is possible that the C-terminal region of *XPO5* contributes to the binding of the pre-miRNA fragment that is not contained in the above mentioned crystal structure, because that section of the pre-miRNA is missing in the reconstituted complex. In fact, the structure deposited in the Protein Data Bank (pdb 3A6P) shows that the C-terminal region is close to the place where the rest of the RNA molecule should be positioned. Alternatively, the cargo-binding defect observed in *XPO5*^{Mut} might be associated with a destabilization of the high-affinity conformation of *XPO5* for pre-miRNA binding, which is also consistent with our band-shift and isothermal titration microcalorimetry data. Further research is warranted in this area.

Interestingly, from a potential translational point of view, the exogenous introduction of wild-type *XPO5* in mutant cancer cells is able to restore the physiological nuclear export of pre-miRNAs, and this *XPO5* functional recovery is associated with tumor growth inhibition properties. Most importantly, *XPO5* transfection in mutant cells caused upregulation of miRNAs with well-characterized tumor-suppressor features, such as the miR-200 family, let-7a, and miR-26a, a finding that might encourage the development of further strategies to restore the expression of miRNAs with tumor-suppressor activities. The development of more efficient delivery systems, such as adeno-associated virus (AAV) vectors, has enabled significant achievements in this area. For example, systemic AAV-mediated delivery of miR-26a in a hepatocellular carcinoma mouse model results in the remarkable suppression of tumorigenesis without evident toxicity (Kota et al., 2009).

In conclusion, we provide evidence that inactivating mutations of the pre-miRNA nuclear export gene *XPO5* occur in human tumors with microsatellite instability. The *XPO5* mutation causes the trapping of pre-miRNAs in the nucleus and impairs the production of mature miRNAs in cancer cells, a phenotype that is rescued by the reintroduction of the wild-type *XPO5* gene. These findings support a role of *XPO5*, as a candidate haploinsufficient tumor-suppressor gene, and suggest that strategies directed toward stimulating the activity of miRNA processing factors and restoring the production of miRNAs with growth inhibitory activities might have a therapeutic value.

EXPERIMENTAL PROCEDURES

Cell Lines and Primary Tumor Samples

Human colorectal and endometrial cancer cell lines were obtained from the American Type Culture Collection. Human gastric cancer cell lines and Co115 were kindly provided by Dr. Minoru Toyota (First Department of Internal Medicine, Sapporo Medical University, Japan) and Dr. Richard Hamelin (INSERM, Paris, France), respectively. DNA samples from primary tumors (n = 337) were obtained at the time of the clinically indicated surgical procedures. All patients provided informed consent and the study was conducted under the approval of the Institutional Review Boards of Vall d'Hebron University Hospital and Sapporo Medical University.

RNA Isolation, Quantification of miRNAs by Real-Time PCR and miRNA Expression Microarray

Total RNA was isolated by Trizol (Invitrogen, San Diego, CA). Extraction was carried out according to the manufacturer's instructions. Nuclear and

cytoplasmic RNA were extracted using the Cytoplasmic and Nuclear RNA purification kit from NORGEN following the manufacturer's instructions. All RNA samples were DNase-treated (Turbo DNA-free, Ambion, Austin, TX). Taq-Man miRNA assays were used to quantify the level of mature miRNAs, as previously described (Melo et al., 2009). Pre-miRNAs processing efficiency calculations are provided in Supplemental Experimental Procedures. The miRNA expression study by microarray analysis was developed as previously described (Melo et al., 2009). Supplemental Experimental Procedures provide further details.

Plasmids, Protein Purification, and Protein Analysis

Protein blotting and confocal microscopy were developed as described in Supplemental Experimental Procedures. The pcDNA3.1+XPO5^{WT}, pcDNA3.1+XPO5^{Mut}, pcDNA3.1+XPO5^{Del.A(A)7}, and pcDNA3.1+XPO5^{Del.A(A)4} expression plasmids were obtained as described in Supplemental Experimental Procedures. GST-Ran, XPO5^{WT}-His₆, XPO5^{Mut}-His₆, and XPO5^{Δ108}-His₆ were expressed in *E. coli* BL21 (DE3) strain. GST fusion Ran was purified on a glutathione-Sepharose column (Amersham Biosciences) and eluted with 50 mM reduced glutathione. Polyhistidine-tagged proteins were purified using nickel-chelating beads (Millipore) and eluted with 200 mM imidazole. Ran/XPO5 interaction and western blot analysis (monoclonal anti-His-Tag 1:1000, Abcam; monoclonal anti-His-Tag biotin conjugated 1:2000) were done as described (Ching et al., 2006). Electrophoretic mobility shift assay was done as described (Yi et al., 2003).

Transfection and Luciferase Assays

pcDNA3.1+pcDNA3.1+XPO5^{WT}, pcDNA3.1+XPO5^{Mut}, pcDNA3.1+XPO5^{Del.A(A)7}, pcDNA3.1+XPO5^{Del.A(A)}, pRS-shXPO5, pGFP, pRS-shGFP, pRS-GFP-empty vector, and pRS-GFPneo-miR-15-16 expression plasmids were transfected by electroporating 6⁷ cells in 0.4 ml PBS with 20 μg of the expression plasmid at 250 V and 975 μF. Stable clones expressing XPO5^{WT} and XPO5^{Mut} were selected in complete DMEM medium supplemented with 1 mg ml⁻¹ G418. Stable clones expressing GFP, miR-15/16, shXPO5, and shGFP were selected in complete DMEM medium supplemented with 0.5 μg ml⁻¹ puromycin. For the luciferase reporter experiments pGL3_Bcl2^{WT} vector (Calin et al., 2008) was used in pRS-GFPneo-miR-15-16 stably transfected cell lines according to the manufacturer's instructions (Promega).

Cell Viability, Colony Formation Assay, and In Vivo Nude Mouse Tumor-Growth Assay

Cell viability was determined by the 3-(4,5-dimethyl-2-thiazolyl)-2,5-diphenyl-2H-tetrazolium bromide (MTT) assay. For colony formation experiments, stable G418, Puromycin and G418 + Puromycin-resistant colonies were fixed and stained with MTT reagent. In vivo nude mouse tumor-growth assays were developed as described in Supplemental Experimental Procedures. All animal experiments were approved by the Bellvitge Biomedical Research Institute (IDIBELL) Ethical Committee and performed in accordance with the guidelines stated in The International Guiding Principles for Biomedical Research involving Animals, developed by the Council for International Organizations of Medical Sciences (CIOMS).

ACCESSION NUMBERS

miRNA-chip data have been deposited into ArrayExpress under accession number E-MTAB-160.

SUPPLEMENTAL INFORMATION

Supplemental Information includes Experimental Procedures, six figures, and one table and can be found online at doi:10.1016/j.ccr.2010.09.007.

ACKNOWLEDGMENTS

Supported by Grant PI08-1345, Consolider MEC09-05, and Dr. Josef Steiner Cancer Research Foundation. S.A.M. is a research fellow of the FCT-Foundation Science and Technology Portugal SFRH/BD/15900/2005 GABBA 2005 PhD program. G.A.C. is supported by The University of Texas M.D. Anderson

Research Trust, University of Texas System Regents Research Scholar, Ladjvardian Regents Research Scholar Fund, and NIH grant 1R01CA135444.

Received: January 20, 2010

Revised: May 28, 2010

Accepted: August 18, 2010

Published: October 18, 2010

REFERENCES

- Bartel, D.P. (2004). MicroRNAs: genomics, biogenesis, mechanism, and function. *Cell* 116, 281–297.
- Bernstein, E., Kim, S.Y., Carmell, M.A., Murchison, E.P., Alcorn, H., Li, M.Z., Mills, A.A., Elledge, S.J., Anderson, K.V., and Hannon, G.J. (2003). Dicer is essential for mouse development. *Nat. Genet.* 35, 215–217.
- Bohnsack, M.T., Regener, K., Schwappach, B., Saffrich, R., Paraskeva, E., Hartmann, E., and Görlich, D. (2002). Exp5 exports eEF1A via tRNA from nuclei and synergizes with other transport pathways to confine translation to the cytoplasm. *EMBO J.* 21, 6205–6215.
- Bohnsack, M.T., Czaplinski, K., and Gorlich, D. (2004). Exportin 5 is a Ran-GTP-dependent dsRNA-binding protein that mediates nuclear export of pre-miRNAs. *RNA* 10, 185–191.
- Brownawell, A.M., and Macara, I.G. (2002). Exportin-5, a novel karyopherin, mediates nuclear export of double-stranded RNA binding proteins. *J. Cell Biol.* 156, 53–64.
- Burk, U., Schubert, J., Wellner, U., Schmalhofer, O., Vincan, E., Spaderna, S., and Brabletz, T. (2008). A reciprocal repression between ZEB1 and members of the miR-200 family promotes EMT and invasion in cancer cells. *EMBO Rep.* 9, 582–589.
- Calado, A., Treichel, N., Müller, E.C., Otto, A., and Kutay, U. (2002). Exportin-5 mediated nuclear export of eukaryotic elongation factor 1A and tRNA. *EMBO J.* 21, 6216–6224.
- Calin, G.A., and Croce, C.M. (2006). MicroRNA signatures in human cancers. *Nat. Rev. Cancer* 6, 857–866.
- Calin, G.A., Liu, C.G., Ferracin, M., Hyslop, T., Spizzo, R., Sevignani, C., Fabbri, M., Cimmino, A., Lee, E.J., Wojcik, S.E., et al. (2007). Ultraconserved regions encoding ncRNAs are altered in human leukemias and carcinomas. *Cancer Cell* 12, 215–229.
- Calin, G.A., Cimmino, A., Fabbri, M., Ferracin, M., Wojcik, S.E., Shimizu, M., Taccioli, C., Zanesi, N., Garzon, R., Aqeilan, R.I., et al. (2008). MiR-15a and miR-16-1 cluster functions in human leukemia. *Proc. Natl. Acad. Sci. USA* 105, 5166–5171.
- Chang, T.C., and Mendell, J.T. (2007). microRNAs in vertebrate physiology and human disease. *Annu. Rev. Genomics Hum. Genet.* 8, 215–239.
- Chang, T.C., Yu, D., Lee, Y.S., Wentzel, E.A., Arking, D.E., West, K.M., Dang, C.V., Thomas-Tikhonenko, A., and Mendell, J.T. (2008). Widespread microRNA repression by Myc contributes to tumorigenesis. *Nat. Genet.* 40, 43–50.
- Ching, Y.P., Chan, S.F., Jeang, K.T., and Jin, D.Y. (2006). The retroviral oncoprotein Tax targets the coiled-coil centrosomal protein TAX1BP2 to induce centrosome overduplication. *Nat. Cell Biol.* 8, 717–724.
- Cummins, J.M., He, Y., Leary, R.J., Pagliarini, R., Diaz, L.A., Jr., Sjoblom, T., Barad, O., Bentwich, Z., Szafranska, A.E., Labourier, E., et al. (2006). The colorectal microRNAome. *Proc. Natl. Acad. Sci. USA* 103, 3687–3692.
- Esquela-Kerscher, A., and Slack, F.J. (2006). Oncomirs—microRNAs with a role in cancer. *Nat. Rev. Cancer* 6, 259–269.
- Gaur, A., Jewell, D.A., Liang, Y., Ridzon, D., Moore, J.H., Chen, C., Ambros, V.R., and Israel, M.A. (2007). Characterization of microRNA expression levels and their biological correlates in human cancer cell lines. *Cancer Res.* 67, 2456–2468.
- Hammond, S.M. (2007). MicroRNAs as tumor suppressors. *Nat. Genet.* 39, 582–583.
- He, L., and Hannon, G.J. (2004). MicroRNAs: small RNAs with a big role in gene regulation. *Nat. Rev. Genet.* 5, 522–531.

- Hill, D.A., Ivanovich, J., Priest, J.R., Gurnett, C.A., Dehner, L.P., Desruisseau, D., Jarzembowski, J.A., Wikenheiser-Brokamp, K.A., Suarez, B.K., Whelan, A.J., et al. (2009). DICER1 mutations in familial pleuropulmonary blastoma. *Science* 325, 965.
- Karube, Y., Tanaka, H., Osada, H., Tomida, S., Tatematsu, Y., Yanagisawa, K., Yatabe, Y., Takamizawa, J., Miyoshi, S., Mitsudomi, T., and Takahashi, T. (2005). Reduced expression of Dicer associated with poor prognosis in lung cancer patients. *Cancer Sci.* 96, 111–115.
- Kim, V.N. (2004). MicroRNA precursors in motion: exportin-5 mediates their nuclear export. *Trends Cell Biol.* 14, 156–159.
- Köhler, A., and Hurt, E. (2007). Exporting RNA from the nucleus to the cytoplasm. *Nat. Rev. Mol. Cell Biol.* 8, 761–773.
- Kota, J., Chivukula, R.R., O'Donnell, K.A., Wentzel, E.A., Montgomery, C.L., Hwang, H.W., Chang, T.C., Vivekanandan, P., Torbenson, M., Clark, K.R., et al. (2009). Therapeutic microRNA delivery suppresses tumorigenesis in a murine liver cancer model. *Cell* 137, 1005–1017.
- Kumar, M.S., Lu, J., Mercer, K.L., Golub, T.R., and Jacks, T. (2007). Impaired microRNA processing enhances cellular transformation and tumorigenesis. *Nat. Genet.* 39, 673–677.
- Kumar, M.S., Pester, R.E., Chen, C.Y., Lane, K., Chin, C., Lu, J., Kirsch, D.G., Golub, T.R., and Jacks, T. (2009). Dicer1 functions as a haploinsufficient tumor suppressor. *Genes Dev.* 23, 2700–2704.
- Lambertz, I., Nittner, D., Mestdagh, P., Denecker, G., Vandesompele, J., Dyer, M.A., and Marine, J.C. (2010). Monoallelic but not biallelic loss of Dicer1 promotes tumorigenesis in vivo. *Cell Death Differ.* 17, 633–641.
- Lee, M.S., Henry, M., and Silver, P.A. (1996). A protein that shuttles between the nucleus and the cytoplasm is an important mediator of RNA export. *Genes Dev.* 10, 1233–1246.
- Lee, Y., Jeon, K., Lee, J.T., Kim, S., and Kim, V.N. (2002). MicroRNA maturation: stepwise processing and subcellular localization. *EMBO J.* 21, 4663–4670.
- Lee, E.J., Baek, M., Gusev, Y., Brackett, D.J., Nuovo, G.J., and Schmittgen, T.D. (2008). Systematic evaluation of microRNA processing patterns in tissues, cell lines, and tumors. *RNA* 14, 35–42.
- Lu, J., Getz, G., Miska, E.A., Alvarez-Saavedra, E., Lamb, J., Peck, D., Sweet-Cordero, A., Ebert, B.L., Mak, R.H., Ferrando, A.A., et al. (2005). MicroRNA expression profiles classify human cancers. *Nature* 435, 834–838.
- Lujambio, A., Ropero, S., Ballestar, E., Fraga, M.F., Cerrato, C., Setien, F., Casado, S., Suarez-Gauthier, A., Sanchez-Cespedes, M., Git, A., et al. (2007). Genetic unmasking of an epigenetically silenced microRNA in human cancer cells. *Cancer Res.* 67, 1424–1429.
- Lund, E., Guttinger, S., Calado, A., Dahlberg, J.E., and Kutay, U. (2004). Nuclear export of microRNA precursors. *Science* 303, 95–98.
- Markowitz, S., Wang, J., Myeroff, L., Parsons, R., Sun, L., Lutterbaugh, J., Fan, R.S., Zborowska, E., Kinzler, K.W., Vogelstein, B., et al. (1995). Inactivation of the type II TGF-beta receptor in colon cancer cells with microsatellite instability. *Science* 268, 1336–1338.
- Medina, P.P., and Slack, F.J. (2008). microRNAs and cancer: an overview. *Cell Cycle* 7, 2485–2492.
- Melo, S.A., Ropero, S., Moutinho, C., Aaltonen, L.A., Yamamoto, H., Calin, G.A., Rossi, S., Fernandez, A.F., Carneiro, F., Oliveira, C., et al. (2009). A TARBP2 mutation in human cancer impairs microRNA processing and DICER1 function. *Nat. Genet.* 41, 365–370.
- Merritt, W.M., Lin, Y.G., Han, L.Y., Kamat, A.A., Spannuth, W.A., Schmandt, R., Urbauer, D., Pennacchio, L.A., Cheng, J.F., Nick, A.M., et al. (2008). Dicer, Drosha, and outcomes in patients with ovarian cancer. *N. Engl. J. Med.* 359, 2641–2650.
- Mohr, D., Frey, S., Fischer, T., Güttler, T., and Görlich, D. (2009). Characterisation of the passive permeability barrier of nuclear pore complexes. *EMBO J.* 28, 2541–2553.
- Okada, C., Yamashita, E., Lee, S.J., Shibata, S., Katahira, J., Nakagawa, A., Yoneda, Y., and Tsukihara, T. (2009). A high-resolution structure of the pre-microRNA nuclear export machinery. *Science* 326, 1275–1279.
- Rampino, N., Yamamoto, H., Ionov, Y., Li, Y., Sawai, H., Reed, J.C., and Peruchio, M. (1997). Somatic frameshift mutations in the BAX gene in colon cancers of the microsatellite mutator phenotype. *Science* 275, 967–969.
- Saito, Y., Liang, G., Egger, G., Friedman, J.M., Chuang, J.C., Coetzee, G.A., and Jones, P.A. (2006). Specific activation of microRNA-127 with downregulation of the proto-oncogene BCL6 by chromatin-modifying drugs in human cancer cells. *Cancer Cell* 9, 435–443.
- Schmittgen, T.D., Jiang, J., Liu, Q., and Yang, L. (2004). A high-throughput method to monitor the expression of microRNA precursors. *Nucleic Acids Res.* 32, e43. 10.1093/nar/gnh040.
- Smith, A.E., Slepchenko, B.M., Schaff, J.C., Loew, L.M., and Macara, I.G. (2002). Systems analysis of Ran transport. *Science* 295, 488–491.
- Spizzo, R., Nicoloso, M.S., Croce, C.M., and Calin, G.A. (2009). SnapShot: microRNAs in cancer. *Cell* 137, 586.
- Thomson, J.M., Newman, M., Parker, J.S., Morin-Kensicki, E.M., Wright, T., and Hammond, S.M. (2006). Extensive post-transcriptional regulation of microRNAs and its implications for cancer. *Genes Dev.* 20, 2202–2207.
- Todorova, R. (2009). Estimation of methods of protein delivery into mammalian cells—a comparative study by electroporation and Biporter assay. *Appl. Biochem. Microbiol.* 45, 493–496.
- Volinia, S., Calin, G.A., Liu, C.G., Ambs, S., Cimmino, A., Petrocca, F., Visone, R., Iorio, M., Roldo, C., Ferracin, M., et al. (2006). A microRNA expression signature of human solid tumors defines cancer gene targets. *Proc. Natl. Acad. Sci. USA* 103, 2257–2261.
- Yi, R., Qin, Y., Macara, I.G., and Cullen, B.R. (2003). Exportin-5 mediates the nuclear export of pre-microRNAs and short hairpin RNAs. *Genes Dev.* 17, 3011–3016.
- Zeng, Y., and Cullen, B.R. (2004). Structural requirements for pre-microRNA binding and nuclear export by Exportin 5. *Nucleic Acids Res.* 32, 4776–4785.
- Zhang, L., Huang, J., Yang, N., Greshock, J., Megraw, M.S., Giannakakis, A., Liang, S., Naylor, T.L., Barchetti, A., Ward, M.R., et al. (2008). microRNAs exhibit high frequency genomic alterations in human cancer. *Proc. Natl. Acad. Sci. USA* 103, 9136–9141.